International Immunopharmacology 132 (2024) 111919

Contents lists available at ScienceDirect

International Immunopharmacology

journal homepage: www.elsevier.com/locate/intimp

PD-1 Receptor (+) T cells are associated with the efficacy of the combined treatment with regulatory t cells and rituximab in type 1 diabetes children via regulatory t cells suppressive activity amelioration

Maciej Zieliński [a,b,1], Justyna Sakowska [a,b,1], Dorota Iwaszkiewicz-Grześ [a,b], Mateusz Gliwiński [a,b], Matylda Hennig [c], Magdalena Żalińska [c,1], Anna Wołoszyn-Durkiewicz [c], Anna Jaźwińska-Curyłło [d], Halla Kamińska [e], Radosław Owczuk [f], Wojciech Młynarski [g], Przemysława Jarosz-Chobot [e], Artur Bossowski [h], Agnieszka Szadkowska [i], Wojciech Fendler [i], Iwona Beń-Skowronek [j], Agata Chobot [k], Małgorzata Myśliwiec [b,c], Janusz Siebert [l], Natalia Marek-Trzonkowska [b,l,m], Piotr Trzonkowski [a,b,*]

[a] Department of Medical Immunology, Medical University of Gdańsk, Debinki 7 80-210, Poland
[b] Poltreg S.A., Botaniczna 20 Street, 80-298 Gdańsk, Poland
[c] Department of Pediatric Diabetology and Endocrinology, Medical University of Gdańsk, Debinki 7 80-210, Poland
[d] Regional Center of Blood Donation and Treatment, Hoene-Wrońskiego 4, 80-210 Gdańsk, Poland
[e] Department of Children's Diabetology, Medical University of Silesia, Medykow 16, 40-752 Katowice, Poland
[f] Department of Anaesthesiology and Critical Care, Medical University of Gdańsk, Debinki 7 80-210, Poland
[g] Department of Paediatrics, Oncology and Haematology, Medical University of Lodz, Sporna 36/50, 91-738 Lodz, Poland
[h] Department of Peadiatrics, Endocrinology, Diabetology with Cardiology Division, Medical University of Bialystok, Jana Kilińskiego 1, 15-089 Białystok, Poland
[i] Department of Pediatrics, Diabetology, Endocrinology and Nephrology, Medical University of Lodz, Sporna 36/50, 91-738 Lodz, Poland
[j] Dept. Pediatric Endocrinology and Diabetology, Medical University of Lublin, ul. Prof. A. Gebali 6, 20-093 Lublin, Poland
[k] Department of Paediatrics, Institute of Medical Sciences, University of Opole, Al. Witosa 26, 45-401 Opole, Poland
[l] Department of Family Medicine, Laboratory of Immunoregulation and Cellular Therapies, Medical University of Gdańsk, Debinki 2 80-210, Poland
[m] International Centre for Cancer Vaccine Science, University of Gdańsk, Wita Stwosza 63, 80-308 Gdańsk, Poland

ARTICLE INFO

Keywords:
Type 1 diabetes
Cell-based therapy
Immune-tolerance
Regulatory T cells
Rituximab
PD-1

ABSTRACT

An imbalance between exaggerated autoaggressive T cell responses, primarily CD8 + T cells, and impaired tolerogenic mechanisms underlie the development of type 1 diabetes mellitus. Disease-modifying strategies, particularly immunotherapy focusing on FoxP3 + T regulatory cells (Treg), and B cells facilitating antigen presentation for T cells, show promise. Selective depletion of B cells may be achieved with an anti-CD20 monoclonal antibody (mAb).

In a 2-year-long flow cytometry follow-up, involving 32 peripheral blood T and B cell markers across three trial arms (Treg + rituximab N = 12, Treg + placebo N = 13, control N = 11), we observed significant changes. PD-1 receptor (+) CD4 + Treg, CD4 + effector T cells (Teffs), and CD8 + T cell percentages increased in the combined regimen group by the end of follow-up. Conversely, the control group exhibited a notable reduction in PD-1 receptor (+) CD4 + Teff percentages.

Considering clinical endpoints, higher PD-1 receptor (+) expression on T cells correlated with positive responses, including a higher mixed meal tolerance test AUC, and reduced daily insulin dosage. PD-1 receptor (+) T cells emerged as a potential therapy outcome biomarker. In vitro validation confirmed that successful Teff suppression was associated with elevated PD-1 receptor (+) Treg levels. These findings support PD-1 receptor (+)

Abbreviations: AUC, area under curve statistics; BMI, body mass index; DDI/kg b.w., daily doses of insulin per kg of body weight; DM1, diabetes mellitus type 1; HC, healthy controls; MMTT, mixed meal tolerance test; NRP-1, Neuropilin-1; PD-1 receptor (+), programmed cell death protein 1; PD-L1, programmed cell death 1 ligand 1; Teff, CD4+ T cells; Treg, regulatory T cells.

* Corresponding author at: Medical University of Gdansk, Department of Medical Immunology, Debinki 7 street, 80-210 Gdansk, Poland
E-mail address: ptrzon@gumed.edu.pl (P. Trzonkowski).

[1] These authors contributed equally to this work.

https://doi.org/10.1016/j.intimp.2024.111919
Received 10 November 2023; Received in revised form 19 March 2024; Accepted 20 March 2024

T cells as a reliable indicator of treatment with combined immunotherapy consisting of Tregs and anti-CD20 mAb efficacy in type 1 diabetes mellitus.

1. Introduction

Both clinical and laboratory data have already proved the importance of the immune system in the pathogenesis of type 1 diabetes mellitus (DM1). While a viral infection or genetic susceptibility may be a triggering factor, the disease develops due to an imbalance between exaggerated autoaggressive T cell responses and impaired tolerogenic mechanisms [1,2].

The most promising disease-modifying strategies are therefore being created around immunotherapy [3,4]. Only recently has teplizumab been introduced, the first-in-century FDA-approved drug for the treatment of presymptomatic DM1 individuals. It is a monoclonal antibody targeting autoreactive CD3 + T cells which allows to get at least a two-year delay in the onset of symptomatic DM1 [5]. Among many ongoing attempts to stop or at least delay DM1, cell therapy with FoxP3 + T regulatory cells (Treg) seems to be of particular interest. Both our and other teams performed several clinical trials with T-regulatory cell products with promising results [6,7,8,9,10].

The major challenge for all these therapies is an excellent immune marker to predict the treatment response, which correlates with β-cell destruction leading to DM1 [11]. The tissue available for sampling is usually peripheral blood, which is very distant from local tissue lesions. Thus, the function of β-cells has remained the only acceptable endpoint of therapeutic efficacy so far [4]. Unfortunately, this sort of monitoring enables us to detect the disease relatively late when the destruction of the islets has already occurred. It shows only the progression of DM1 and does not allow to predict treatment efficacy early enough, preferably at the time of therapy.

This study aimed to identify and validate biomarker candidates for immune intervention in DM1 in our clinical trial TregVAC2.0 (clinical trial registration ISRCTN37116985). We assessed cellular and humoral immunity in newly diagnosed DM1 patients treated with combined therapy of autologous polyclonal CD3 + CD4 + $CD25^{high}CD127$- T regulatory cells and anti-CD20 antibody (Tregs + RTX group) as compared to the patients treated with polyclonal Treg administration only (Tregs group) or standard-of-care treatment with insulin (control group). We expected, as a final result, to find a marker or markers in the immune system which would correlate with β-cell function and could be employed to predict the response to the immunotherapy during the trial (Fig. 1).

2. Materials and methods

2.1. Study design

It was a phase 1/2, prospective, multicenter clinical trial to study treatment efficacy and impact on selected immune parameters of combined therapy with autologous Treg administration and anti-CD20

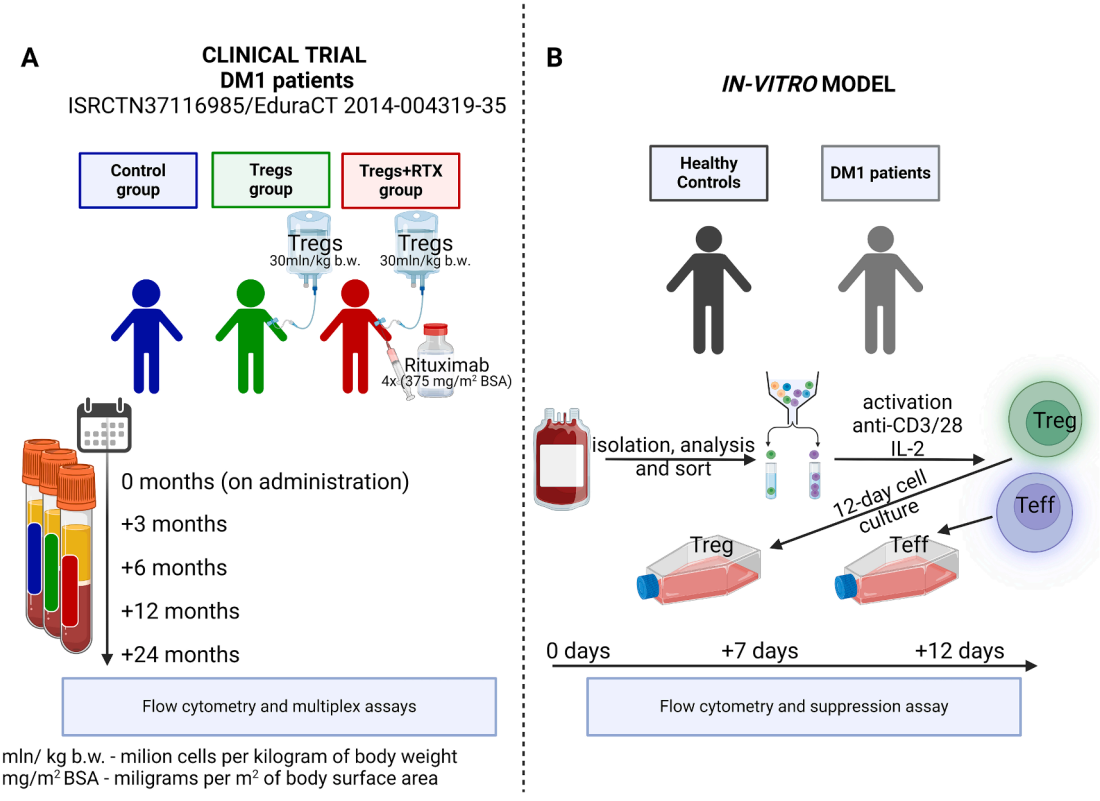

Fig. 1. Study flow diagram for the clinical trial and in-vitro model experiment. In the clinical trial EudraCT 2014-004319-35 and ISRCTN37116985 (left panel), three groups of newly diagnosed DM1 patients are compared: standard therapy (blue), autologous Treg (green), and autologous Treg with rituximab (red). Tregs are administered twice, at the beginning of the clinical trial and three months after it (30×10^6 cells/kg of body weight each), while rituximab is administered in 4 doses (375 mg/m^2 of body surface area) over 1 month following the first dosage of Treg. Patients are followed up, and samples for immunophenotyping and multiplexing are collected on administration, and three, six, twelve, and twenty-four months after. In the in vitro experiment (right panel), healthy controls and newly diagnosed DM1 patients are assessed. Sorted Treg and T effector cells are stimulated with CD28/CD3 beads in the IL-2 enriched cell culture medium for 12 days. The immunophenotyping and the suppression tests are carried out from PBMCs and then on day seven and twelve of Treg and Teff culture.

Table 1A
Clinical trial participant's patient's baseline characteristics.

Characteristics	Treg + placebo [Treg] (n = 13) mean ± SD	Treg + rituximab [Tregs + RTX] (n = 12) mean ± SD	Control (n = 11) mean ± SD	p-value
Male gender, n (%)	7 (52.8)	5 (41.7 %)	5 (45.5)	0.61
Age, years	13.3 ± 1.5	12.9 ± 1.2	12.1 ± 2.2	0.68
Body mass index., kg/m^2	19.57 ± 1.8	18.1 ± 1.8	18.4 ± 1.4	0.45
Body mass index, Z-core	–0.24 ± 0.46	–0.01 ± 0.43	0.04 ± 0.42	0.19
Ethnicity, Caucasian (%)	13 (100.0)	12 (100.0)	11 (100.0)	–
Months since diagnosis	6.5 ± 4.2	6.0 ± 4.2	5.0 ± 3.2	0.48
Insulin (TDD per kg of body weight)	0.3 ± 0.3	0.2 ± 0.2	0.3 ± 0.3	0.71
C-peptide				
Fasting C-peptide (μg/L)	1.1 ± 0.4	1.1 ± 0.3	0.98 ± 0.2	0.45
*Stimulated C-peptide AUC240 (h*μg/L)*	10.1 ± 2.4	11.0 ± 3.7	9.8 ± 2.1	0.38
Glycated haemoglobin (%)	6.3 ± 1.1	6.6 ± 1.2	6.6 ± 0.8	0.72
Glucose (mg/dl) (a mean value from fasting seven days before the visit)	103.1 ± 9.7	109.5 ± 13.5	103.9 ± 13.3	0.55
Autoantibodies				
Glutamic acid decarboxylase (IU/ml)	856.6 ± 936.5	381.0 ± 594.6	744.2 ± 768.1	0.74
Insulin autoantibody (IU/ml)	8.7 ± 8.6	5.3 ± 5.5	5.0 ± 5.1	0.38
Islet cell antibody (titre)	109.2 ± 180.5	125.0 ± 185.0	50.9 ± 47.6	0.25

P-values are based on one-way ANOVA F-statistics for continuous and Kruskal-Wallis statistics for multilevel categorical data; adapted from [7] [7] The TDD per kg of body weight stands for insulin total daily dose per kg of body weight.

Table 1B
DM1 in-vitro model patient's baseline characteristics.

Characteristics	Type 1 diabetes patients [DM1] (n = 12) mean ± SD	Healthy controls [HC] (n = 12) mean ± SD	p-value
Male gender, n (%)	9 (75)	10 (83.3)	>0.99
Age, years	11.6 ± 2.8	29.8 ± 6.1	<0.0001
Ethnicity, Caucasian (%)	12 (100.0)	12 (100.0)	not applicable
Body mass index, kg/m^2	18.24 ± 1.74	—	not applicable
Insulin (TDD per kg of body weight)	0.09 ± 0.10	—	not applicable
Glycated haemoglobin (%)	6.30 ± 0.99	—	not applicable
Fasting C-peptide (μg/L)	1.02 ± 0.54	—	not applicable

The p-values are based on Fisher's exact test for categorical data and the *t*-test for continuous data. Healthy controls were anonymous blood donors, all characteristics were assumed to be within normal range, n/a – not applicable. The TDD per kg of body weight stands for insulin's total daily dose per kg of body weight.

monoclonal antibodies in children and adolescents with recently diagnosed DM1. The study was a prospective, open-label and randomised 24-month-long clinical trial registered as ISRCTN37116985 and EudraCT 2014-004319-35. In this three-arm trial, the follow-up was performed in a standard-of-care control group (control; 11 patients), the group treated with autologous polyclonal Treg only (Tregs; 12 patients), and the group treated with combined therapy with autologous polyclonal Treg and anti-CD20 antibodies (Tregs + RTX; 13 patients). Interventional groups, which consisted of Tregs + RTX and Tregs patients, received two doses of Treg in an open-label manner, 30x10^6 cells/kg b.w. per dose, three months apart starting from day 0. The administration of the anti-CD20 antibody was blinded and placebo-controlled. The patients were randomly assigned to an anti-CD20 antibody or placebo by the element of chance (coin) to receive four dosages of rituximab (375 mg/m^2 of body surface area; Tregs + RTX group) or placebo (Tregs group) on +14, +22, +29, and +36 days of the trial. All the participants were followed up for two years posttherapy and assessed at administration, three, six, twelve, and twenty-four months after, as given in the study flow diagram (Fig. 1A). The report on the efficacy and safety of combined therapy drawn up in this clinical trial has already been published. We proved that the combined autologous Treg administration and anti-CD20 antibodies therapy was superior to the Treg administration-only treatment in DM1, as assessed by the AUC of C-peptide mixed meal tolerance test and the percentage of patients in clinical remission 24 months after the trial. The therapy was safe, despite the 80 % adverse events rate in Tregs + RTX patients, as no adverse event led either to withdrawal of medical intervention or the patient's death [7].

The current study aimed to assess the immune imprint in DM1 individuals. In a two-year follow-up, we set multicolour immunophenotypes of CD4 + Treg, CD4 + Teff and CD8 + T cells, trying to correlate them with the clinical and laboratory outcomes. Likewise, immune correlations were analysed in humoral immunity and cytokine milieu. The results were then matched with the in-vitro model of the Treg and CD4 + Teff cell cultures from DM1 patients and healthy volunteers, as given in the study flow diagram (Fig. 1B). Finally, the laboratory findings were correlated with the clinical trial outcomes. The study was approved by an independent institutional review board (NKBBN/374/2012-NKBBN/374–7/2014 for the clinical trial and NKBBN/414/2018 for the in-vitro study) and all participants signed an informed consent form.

2.2. Patients

All the participants were recruited based on the detailed inclusion and exclusion criteria given in the supplementary data Table S1 for both the clinical trial and the in-vitro model. By the power analysis for sample numbers, thirteen patients in the randomised treatment arm were satisfactory to find a 20 % difference in the geometric mean ratio of AUC (0–240 min) of C-peptide (alpha 5 %), a significant outcome of the clinical experiment. In the clinical trial, treated patients (Tregs + RTX and Tregs), were compared with standard-of-care DM patients (control). For the in-vitro model, 12 DM1 patients and 12 healthy controls were enrolled. DM1 patients were selected upon inclusion/exclusion criteria equal to the clinical trial, and healthy controls were blood donors from the Regional Blood Bank in Gdańsk whose buffy coats remained after blood product preparation. The detailed baseline demographics are given in Tables 1A and 1B for the clinical trial and the in-vitro model. In the clinical trial, treated patients (Tregs + RTX and Tregs), were compared with standard-of-care DM patients (DM control), and for the in-vitro model DM patients were compared with healthy control (HC). By this approach, the results can be referred to the unaffected individuals (HC), but also to the DM patients treated only with the insulin-based therapy (DM control).

2.3. Methods

All the cellular assays were carried out on fresh samples, and processed up to 24 h following blood collection. The solid phase assays (cytokines and antibodies) were tested in batches of samples stored at −80 °C.

2.3.1. Cell isolation

The Ficoll Paque Plus (GE Healthcare, Chicago, IL), a density gradient isolation, was used for PBMC isolation from EDTA whole blood from DM1 patients or buffy coats from blood products obtained from

healthy volunteers. The isolated cells were then counted and tested for viability with the Bio-Rad TC20 (Hercules, CA), an automated trypan blue cell viability analyser. The minimum viability cut-off used for testing was 90 %.

2.3.2. Cell sorting and culture for in vitro model of Treg stimulation

CD4 + T cells were isolated from PBMC using a negative immunomagnetic selection kit (EasySep Human CD4 Negative Selection Kit, StemCell Technologies; Vancouver, BC, Canada) and next stained with fluorescence-conjugated monoclonal antibodies (BDBiosciences, Poland): anti-CD3 (clone UCHT1), anti-CD4 (clone SK3), anti-CD25 (clone M−A251), and anti-CD127 (clone HIL-7R-M21). Finally, cells were sorted with FACS Aria II sorter or FACS Influx sorter (BD Bioscience, Franklin Lakes, NJ) into regulatory T cells (Treg), with the phenotype (CD4+/CD25^{high}/CD127-/doublets-) and effector T cells (Teff) with the phenotype (CD4+/CD25^{low}/CD127+/doublets-). Next, the sorted cells were cultured according to our previously published protocol [12,13]. Briefly, cells were suspended in X-Vivo medium (Lonza, Belgium) supplemented with a heat-inactivated autologous serum (DM1 patients) or AB human male serum (healthy controls) and 1 × 10^4-1 × 10^2 UI/ml of IL-2 (Proleukin, NOVARTIS, Germany) for 12 days. Treg and Teff were activated for proliferation with beads coated with anti-CD3 and anti-CD28 antibodies (MACS GMP ExpAct Treg Kit, Miltenyi Biotec, Germany) at day 0 and day 5 in 1:1 bead-to-cell concentration ratio.

2.3.3. Flow cytometry

An extended flow cytometry profile of peripheral lymphocytes was applied to study several immune parameters for the clinical trial groups, as given in the supplementary data Table S2A. Twenty-two markers were analysed using three 16-colour combinations of the fluorochromes. We used minimum backbone markers for gating purposes, which refers to the CD3, CD4, FoxP3, Helios, CD45RA, and CD62L markers. Upon this, Treg, CD4 + Teff, and CD8 + T cells were gated, as shown in the supplementary data Fig. S1A.

Peripheral blood lymphocytes B were gated as CD19/CD20 double positive lymphocytes (backbone markers) and further analysed for the antigens associated with the cell maturation, memory development, and class-switching (Fig. 1SB), as given in Table S2B.

For the in vitro model, a reduced number of parameters was tested due to the limited number of cells (Table S2C). Again gating was carried out upon similar backbone markers, with the previous cells' viability testing (trypan blue), as given in Fig. S1C.

Appropriate isotype controls and fluorescence minus one (FMO) approach were used to gate the population of interest for every analysis. The minimum number of cells per flow cytometry tube was 200.000 ± 20.000 viable cells, and a minimum of 80.000 out of it was collected upon flow cytometry testing with BD LSRFortessa Cell Analyzer (BD Bioscience, Franklin Lakes, NJ).

2.3.4. Suppression assay

Eight DM1 and five healthy control cultures were randomly selected to perform the suppression assays on day seven and day twelve of the culture. The suppressive potential of Tregs was assessed as inhibition of Teff proliferation in the presence of Treg. The 1x10^5 Teff per culture were stained with 1 μM/ml of carboxyfluorescein succinimidyl ester (CFSE) proliferation dye (BD Bioscience, Franklin Lakes, NJ) and cocultured with titrating concentrations of Treg as follows (Teff:Treg) 1:2, 1:1, 1:0.5, 1:0.25, and 1:0.125. Cells were then activated with magnetic beads coated with anti-CD3 and anti-CD28 antibodies (MACS GMP ExpAct Treg Kit, Miltenyi Biotec, Germany) in a 1:1 bead to Teff ratio and cultured for 72 h. The bead-stimulated cultures of Teff without Treg served as a positive control, and the unstimulated cultures of Teff and Treg as a negative control. The fluorescence of CFSE in the samples was acquired with BD LSR Fortessa Cell Analyzer (BD Bioscience, Franklin Lakes, NJ). Results were analysed using the proliferation modelling tool in FlowJo (Ashland, OR) and presented as proliferation index (PI). A representative gating example is given in Fig. S1D.

2.3.5. Flow cytometry data analysis

Several immune parameters of Treg, CD4 + Teff, CD8 + T cells, and B lymphocytes were analysed. First, we screened data using the heatmap approach for each group up to two years of the follow-up. Next, with stochastic analysis of cell phenotype, a further assessment was carried out to find the best fitting parameters which would enable to discriminate treated from control patients. Finally, ANOVA statistics were calculated for the selected parameters to find statistical significance.

The flow cytometry data was analysed using Kaluza Software (Beckman Coulter, Brea, CA) and FlowJo Software (Ashland, OR). First, using backbone markers, significant T and B cell subsets were identified, and the expression of distinct antigens was noted as percentages. Next, data was analysed using FlowJo's Software dimensionality reduction algorithms to find significant cell subpopulations between tested groups. We used t-distributed Stochastic Neighbour Embedding (tSNE) and TriMap algorithms with the following PhenoGraph algorithm, a clustering method for identifying phenotypically distinct subpopulations [14,15,16].

In FlowJo software, starting with the raw FCS files, downsampling was done to reduce the number of events to normalise the population size, and then Treg, CD4 + Teff and CD8 + T cells were gated (Fig. S2A). We used thirty thousand events downsampling regularly across the time order of collected events. Next, normalised Treg, CD4 + Teff and CD8 + T cells subpopulation events from single samples were aggregated into one FCS file (particular condition) for further dimensionality reduction algorithms analysis. The tSNE was done using opt-SNE configuration, setting: iteration = 1000, perplexity = 30, the k nearest neighbours algorithm as a vantage point tree, and Barnes-Hut as a gradient algorithm [14]. The TriMap analysis was carried out with Euclidean distance function, nearest neighbours = 10, and the number of outliers = 5 [15]. Then, the PhenoGraph algorithm was calculated with the k number (the number of nearest neighbours used for the nearest-neighbour graph) suggested by the plugin upon the FCS file structure [16]. Finally, the Cluster Explorer plugin was used to select populations of interest. The detailed analysis protocol is given in the supplementary data Fig. S2B.

2.3.6. Serum immunoglobulins and autoantibodies

The serum concentrations of IgA, IgM immunoglobulins, and IgG subclasses: IgG1, IgG2, IgG3, and IgG4 were measured with Bio-Plex Pro Human Isotyping Panel kit (Bio-Rad, Hercules, CA) according to the manufacturer's protocol and read on Luminex MAGPIX analyser (Merck Millipore; Burlington, MA).

2.3.7. Autoantibodies

Anti-GAD65 (glutamic acid decarboxylase antibodies) and anti-IAA (insulin autoantibodies) antibodies were tested with ELISA (Euroimmun, Germany). Anti-ICA (anti-islet cell antibodies) were tested with indirect immunofluorescence assay (IIF) with primate pancreas as the antigenic substrate (Euroimmun, Germany).

2.3.8. Serum cytokines

The serum concentration of 38 cytokines was measured with the bead-based multiplex assay - Human Cytokine/Chemokine Magnetic Bead Panel, Milliplex (Merck Millipore; Burlington, MA) according to the manufacturer's protocol and read on Luminex MAGPIX analyser (Merck Millipore; Burlington, MA).

2.3.9. Statistic data analysis

Throughout the study, data was expressed as the mean with a standard deviation and only cleaned-up data with the Grubbs test was used for all statistical tests. Due to normal distribution testing, the data was assessed with the use of non-parametric tests.

All between-group comparisons were performed using the

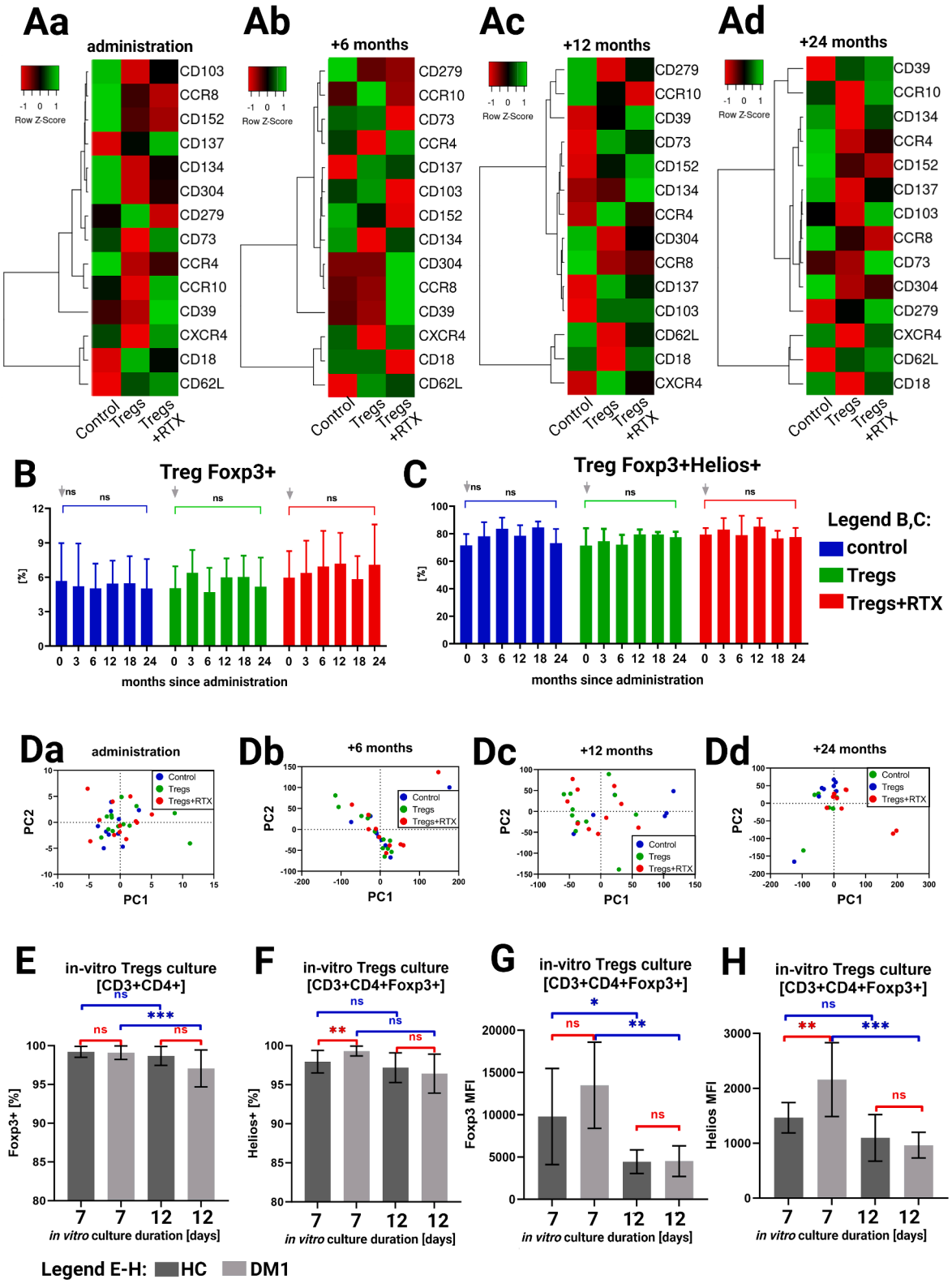

(caption on next page)

Fig. 2. Regulatory T cells phenotype during patient follow-up, compared to the in-vitro model. The heatmaps in **(Aa-Ad)** illustrate the Treg phenotype during patient follow-up in a clinical trial, depicting the lowest expression in red and the highest expression in green. The percentages of FoxP3 + Treg **(B)** and FoxP3 + Helios + Treg **(C)** are tracked on administration, and on three, six, twelve, eighteen, and twenty-four months throughout the clinical trial. "Treg" refers to CD4 + regulatory T cells with FoxP3 intracellular expression, and "Helios + FoxP3+" signifies CD4 + regulatory T cells with both FoxP3 and Helios intracellular expression. Principal component analyses **(Da-Dd)** were conducted on the Treg immunophenotype, comparing three patient groups in the clinical trial. The percentages of FoxP3 + Treg cells **(E)** and the percentages of Helios + FoxP3 + Treg cells **(F)** are assessed in the in-vitro model, comparing healthy controls (HC, dark grey bars) with DM1 patients (light grey bars). Similarly, the relative FoxP3 antigen expression **(G)** and the relative Helios antigen expression **(H)**, measured as MFI (mean fluorescence intensity), are examined in the in-vitro model, comparing HC and DM1 patients. On sub-panel charts, E-H comparisons between groups are made on day seven and day twelve (red) and within group day seven to twelve (blue). In terms of statistical significance, Kruskal-Wallace for multiple comparisons and Mann-Whitney *U* test for comparison of two sets of data are used, and "NS" denotes non-significant, and significant p values are represented as follows: "***" (0.000–0.001), "**" (0.001–0.010), and "*" (0.010–0.050). The arrows denote the comparison between control, Tregs, and Tregs+RTX at administration if light grey. The group numbers are 11/13/12 for control, Tregs, and Tregs+RTX in the clinical trial (sub-panel chart B, C) and 12 for both control and DM1 in the vitro model (sub-panel chart E, F, G, H). For the B, C, and E-H sub-panel charts, the bars represent mean values while the lines a standard deviations. For the sub-panel chart D, the Monte Carlo simulation conducted the Principal components analysis (PCA). The dots represent control (blue), Tregs (green), and Tregs+RTX (red) in the clinical trial, and PC1 and PC2 denote principal component axes. In the sub-panel chart A heatmaps represent selected parameters expressed on the right and colours denote z scores, value −1 in red and value +1 in green.

nonparametric Mann-Whitney *U* test, while Kruskall-Wallace or Welch's ANOVA was applied for multiple data sets. If data was skewed, not Gaussian, the Brown-Forsythe ANOVA test was used. The relationships between data sets were tested with Spearman rank correlations, and the frequency was assessed with the Chi-square test. The visualisation of correlations calculated for several data sets was carried out with colour-coded correlation matrix graphs and XY data points diagrams with 95 % confidence bands of the best-fit line. Principal components analysis (PCA) was conducted through Monte Carlo simulation.

A receiver operating characteristic curve (ROC) was calculated with the Wilson/Brown method and 95 % confidence interval (95 %CI). Data was presented as the mean values, with the standard deviation and visualised with bar graphs. The tops of each bar indicate means, while lines represent standard deviation. Significance was set at $p < 0.05$. The significance code for the p-value was as follows: "***" (0.000–0.001), "**" (0.001–0.010), and "*" (0.010–0.050). All analyses were performed in Prism 9 (GraphPad Software; Boston, MA). The heatmaps were generated with a Heatmapper (https://www.heatmapper.ca/), where average linkage was used as a clustering method and Euclidean as a distance measurement method [17]. Figures were prepared with BioRender.

3. Results

3.1. Treg number, FoxP3 + and Helios transcription factor expression

First, we screened data using the heatmap approach for each group up to two years of follow-up. No significant differences were found between the groups throughout the follow-up (Fig. 2A a-d). Neither FoxP3 + nor FoxP3 + Helios + Treg percentage changed significantly in both control and treated patients. No between-group differences were noted during the 2-year-long monitoring (Fig. 2B, C). With a principal component analysis of FoxP3 + or FoxP3 + Helios + double positive Treg, only 11 – 20 % of differences between treated and control groups were tested from recruitment (Fig. 2Da) up to two years of monitoring (Fig. 2Db, Dc, Dd). Despite high numbers of cells on administration, no persistent lymphocytosis was observed. Post-administration complete blood count (CBC) showed a rapid decline in lymphocyte count and no persistent lymphocytosis [7].

In the in-vitro model of Treg stimulation, compared to a stable percentage in healthy controls (HC), we found a decreasing percentage of FoxP3 + Treg and FoxP3 + Helios + Treg between day seven and day twelve in the cultures of cells from DM1 individuals (Fig. 2E, F). Similarly, the expression (measured as mean fluorescence intensity - MFI) of FoxP3 decreased throughout the culture, while Helios expression declined in the DM1 group only (Fig. 2G, H).

3.2. PD-1 receptor (+), the immune checkpoint antigen

An in-depth analysis revealed that the percentage of PD-1 receptor (+) T cells changed significantly throughout the study, based on tSNE analysis (Fig. 3Aa, Ba, Ca). In the control group, the percentage of PD-1 receptor (+) T effector cells (Teff) gradually decreased from + 6 to + 24 months of the follow-up ($p = 0.02$). Conversely, there were an increasing percentage of PD-1 receptor (+) CD4 + Teff and PD-1 receptor (+) CD8 + T cells in the treated groups throughout the trial; however, it was significant only in the combined treatment Tregs + RTX group (Fig. 3Ab, 3Bb). Hence, there was a considerable difference between the control and combined-treatment groups in the percentage of PD-1 receptor (+) Teff at + 24 months ($p = 0.009$) (Fig. 3Ab, black arrows) and PD-1 receptor (+) CD8 + T cells at + 12 months ($p = 0.04$) (Fig. 3Bb, brown arrows). There were similar trends in the follow-up in the level of PD-1 receptor (+) Treg, but neither the decrease in the control group nor the increase in the treated group reached statistical significance. The only between-group difference for Treg was between control and combined-treatment patients at + 24 months ($p = 0.001$) (Fig. 3Cb, black arrows). In-vitro, compared to healthy controls, a higher percentage of PD-1 receptor (+) Treg and PD-1 receptor (+) Teff was noted in the DM1 group in PBMCs on day 0 ($p = 0.032$ and $p = 0.006$), and PD-1 receptor (+) Treg subsequently increased in the culture in both groups to be comparable at day + 7 ($p = 0.932$) (Fig. 3D, E). Interestingly, on day + 12, the percentage of PD-1 receptor (+) Treg in cultures dropped dramatically in the cultures from DM1 patients and was significantly lower than in the healthy group (Fig. 3D). At the same time, the expression of PD-1 receptor (+) on a per-cell basis measured as MFI was markedly higher in the cultures from DM1 patients than in the ones from healthy controls on day 0, day + 7 and day + 12 (Fig. 3F). No such differences were noted in the cultures of CD4 + Teff (Fig. 3G).

3.3. Treg suppressive activity correlated with the percentage of PD-1 receptor (+) Treg in the DM1 group

The suppressive activity of Treg was tested as an inhibition of the proliferation of Teff in the cocultures of stimulated Teff with autologous Treg. Interestingly, there was a correlation between the percentage of PD-1 receptor (+) Treg and suppression only for the DM1 group on day + 7 ($r = -0.552$; $p = 0.005$) (Fig. 3H). The effect disappeared on day + 12 when the percentage of PD-1 receptor (+) Treg dropped significantly in the DM1 group (Fig. 3D, I). No correlation was observed for healthy controls, neither on day + 7 nor day + 12 (Fig. 3H, I).

3.4. The expression of other biomarker candidates in the follow-up

For Treg and Teff, a gradual drop in the percentage of CD73 + cells was found in control DM1 individuals ($p = 0.003$ and $p = 0.007$, respectively). The patients receiving Tregs or combined treatment did

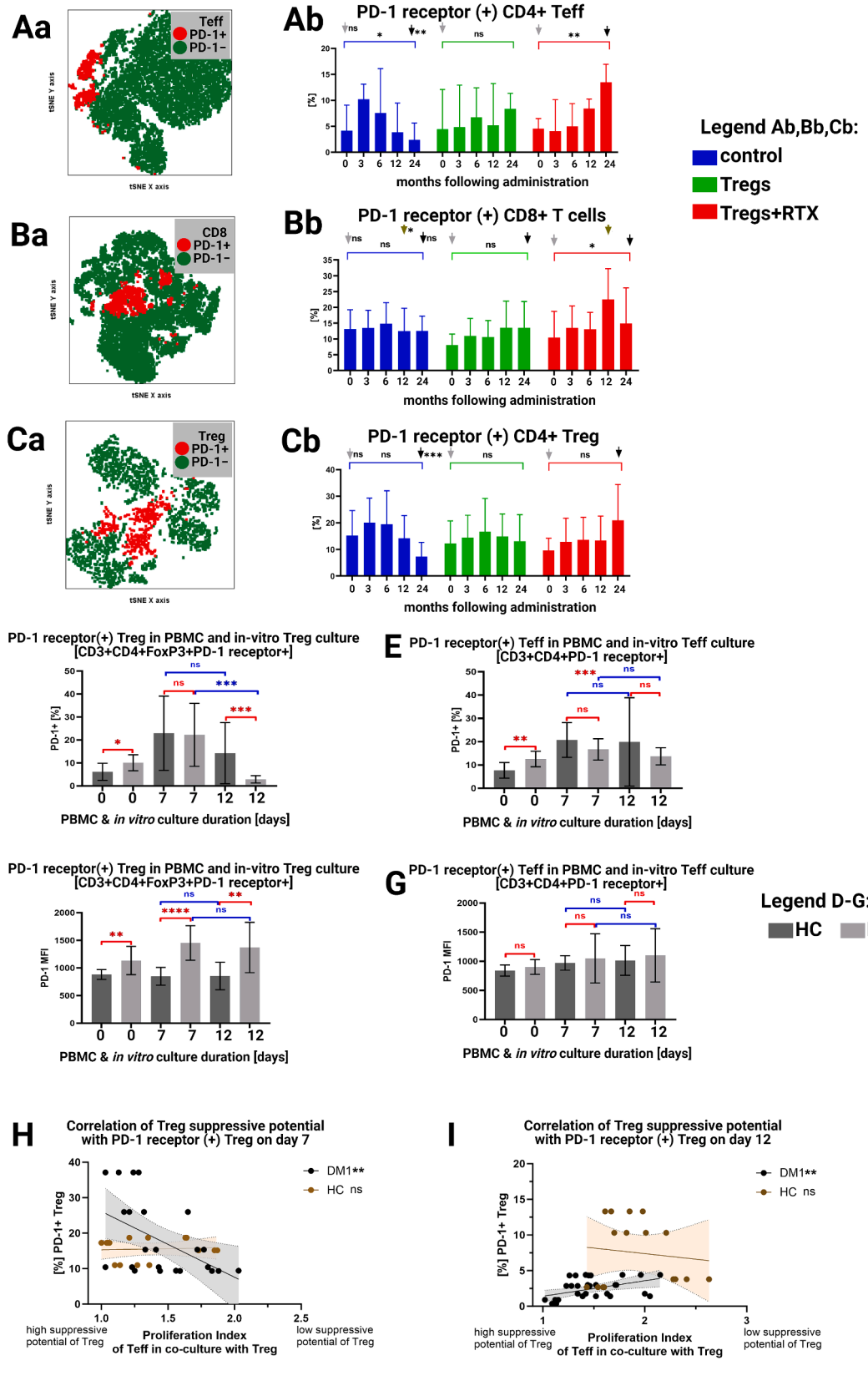

(caption on next page)

Fig. 3. The expression of PD-1 receptor (+) on regulatory T cells and effector T cells during patient follow-up, compared to the in-vitro model. In the right panel **(Aa, Ba, Ca),** representative examples of a tSNE diagram are provided with PD-1 receptor (+) - expressing cells indicated in red colour among PD-1 receptor (+) - negative CD4 + Teff **(Aa),** CD8 + T cells **(Ba),** and Treg cells **(Ca),** respectively. The percentages of PD-1 receptor (+) expression (left panel) on effector T cells **(Ab)**, CD8 + T cells **(Bb)**, and FoxP3 + Treg **(Cb)** are tracked throughout the clinical trial follow-up. "Treg" denotes CD4 + regulatory T cells with FoxP3 intracellular expression, and "Teff' stands for CD4 effector T cells. Statistical comparisons are made on Treg administration (grey arrows), on twenty-four months after (black arrows), or for the highest numbers (brown arrows). The percentages of PD-1 receptor (+) FoxP3 + Treg cells **(D)** and the percentages of PD-1 receptor (+) effector T cells **(E)** in the in-vitro model are compared between healthy controls (HC, dark grey) and DM1 patients (light grey). Similarly, relative PD-1 receptor (+) expression measured as MFI - mean fluorescence intensity on PD-1 receptor (+) FoxP3 + Treg cells **(F)** and relative PD-1 receptor (+) expression on CD4 + Teff cells **(G)** in the in-vitro model are compared between HC and DM1 patients. The time day zero indicates analysis of peripheral blood mononuclear cells (PBMC), and day 7, and day 12 indicate the duration of cell cultures. The comparisons between HC and DM1 are taken at the beginning of the experiment, day seven, and day twelve (red), or within each group days seven to twelve (blue). The effector T cells' suppression test by Treg on day seven **(H)** and twelve **(I)** of the in-vitro experiment is conducted. Treg from HC (n = 5) are represented in brown, and from DM1 (n = 8) in black. The comparison visualises the percentages of PD-1 receptor (+) FoxP3 + Treg cells (y-axis) and the effector T cell's proliferation index (x-axis). Lines indicate a correlation trend and 95 % ellipse's coefficient intervals. In terms of statistical significance, the Kruskal-Wallace for multiple comparisons and Mann-Whitney *U* test for comparison of two groups and the Wilcoxon test for 2 sets of data of the same group are used. For charts H and, I correlations are calculated with a simple linear regression model and non-parametric Spearman correlation. "NS" denotes non-significant, and significant p values are represented as follows: "***" (0.000–0.001), "**" (0.001–0.010), and "*" (0.010–0.050). The arrows denote the comparison between control, Tregs, and Tregs + RTX at administration if light grey, or 24 months after if black, or six months after if brown. The group numbers are 11/13/12 for control, Tregs, and Tregs + RTX in the clinical trial (sub-panel chart A, B, C) and 12 for both control and DM1 in the in vitro model (sub-panel chart D, E, F, G). For the A-G sub-panels charts, the bars represent means and line standard deviations.

not manifest such a decrease ($p > 0.05$) (Figure S3). No differences were found in the percentage of CD39 + Treg or Teff (another enzyme involved in nucleotide metabolism) throughout the trial (Figure S4). Similarly to CD73 + Treg, the percentage of CD304+ (NRP-1 antigen) Helios + Treg decreased in the control group only in the follow-up ($p = 0.02$). Nevertheless, the expression of this biomarker on Treg was low, rarely exceeding 2 % of all Treg (Figure S5). Finally, a significant increase in CD134+ (OX-40 antigen) Helios + Treg percentage was noted in the control group and both interventional arms throughout the follow-up, reaching the highest level in the control group (Figure S6).

3.5. B cell subsets and immunoglobulins

Significant changes in B cell subsets were noted in the Tregs + RTX group only (Fig. 4A). Almost complete depletion of B cells was noticeable in the first six months after injection of the anti-CD20 antibody. At + 12 months, as compared to the baseline, B cell recovery was seen with a significant reduction in the percentage of CD27 + B memory cells ($p < 0.001$) (Fig. 4A-black arrows, 4B). At the same time, the percentage of Breg-like cells (CD38++CD24++) and transitional (CD38 + CD24 +) B cells almost doubled ($p < 0.001$) (Fig. 4A-white arrow, 4Ca, 4 Da). At + 24 months, it dropped to baseline in the case of the former subset, but it remained two-fold for the latter one (Fig. 4C, D).

In addition, a characteristic switch in the IgG1/IG2 index was found in the Tregs + RTX group. A significant decrease in the serum concentration of IgG1 ($p = 0.003$) was noted, with a concomitant increase in the concentration of IgG2 throughout the follow-up (Fig. 4E, F). The levels of IgM were significantly reduced for the entire study up to + 24 months ($p = 0.001$), and the lowest levels were noted at + 6 months of the trial (Fig. 4G). There were no changes in the serum concentrations of IgA (Figure S7). No incidents of late hypogammaglobulinemia were observed one to two years after rituximab treatment for IgA (<0.42 mg/ml) and IgG (IgG1 < 3.16 mg/ml; IgG2 < 0.86 mg/ml; IgG3 < 0.14 mg/ml; IgG4 < 0.01 mg/ml) subclasses [18].

There was also a partial reduction in the serum autoantibodies, like anti-GAD-65 autoantibodies, that decreased significantly in Tregs + RTX patients only ($p < 0.001$). On the contrary, anti-IAA autoantibodies were reduced in all patients at month + 24, while anti-ICA autoantibodies did not change throughout the 24-month-long monitoring (Fig. 4H, I, J).

3.6. The correlation of immune markers and disease progression

The presented immune parameters were subsequently correlated with the clinical outcome results, such as mixed meal tolerance test (MMTT) assessed by area-under-curve of plasma c-peptide concentration (MMTT AUC), glycated haemoglobin (HbA1C), serum c-peptide, and daily dose insulin per kg of body weight (DDI/kg of b. w.). The first screen with the correlation matrix is shown in Figure S8. However, statistically significant correlations are presented in Fig. 5. There was a common correlation of better clinical outcomes with the percentage of PD-1 receptor (+) Treg (Fig. 5A) and PD-1 receptor (+) Teff (Fig. 5B) in both control and treated patients at the end of a two-year-long follow-up. Less commonly, the clinical parameters were correlated with the percentages of CD73 + Treg and CD73 + Teff throughout two years of the follow-up. Interestingly, there was also a correlation between CD304 + Treg and better clinical outcomes (Fig. 5). The values of correlation strength and their significance are summarised in Table 2.

The AUC for a receiver operating characteristic curve (ROC) was calculated for results obtained at the end of the follow-up, and only for Tregs + RTX patients the significant markers were identified as PD-1 receptor (+) Treg, PD-1 receptor (+) Teff, and CD73 + Treg (Table S3). For the cut-off value of > 16 % of PD-1 receptor (+) Treg and > 8 % of PD-1 receptor (+) Teff, the sensitivity was 73 % (43.44 % to 90.25 %; 95 %CI), and 72 % (45.25 % to 89.50 %; 95 %CI) while specificity was 92 % (64.61 % to 99.57 %; 95 %CI), 90 % (70.54 % to 96.28 %; 95 %CI), respectively (Fig. 5C, D). For the percentage of CD73 + Treg for the > 7 % cut-off value, the sensitivity was 82 % (52.30 % to 96.77 %; 95 %CI), and specificity was 83 % (55.20 % to 97.04 %; 95 % CI), (Figure S3).

3.7. The serum cytokine milieu

Serum cytokines were screened with the heatmap approach with no constant pattern in the groups throughout 2 years of the follow-up (Fig. 6A a-d). Interestingly, compared to the control patients, IL-10 serum concentration was two-fold and three-fold higher in Tregs and Tregs + RTX patients, respectively at three months of the follow-up ($p < 0.001$) (Fig. 6B, dark grey arrows). The phenomenon continued for 6 months following recruitment (Fig. 6B, brown arrows). Moreover, IL-10 concentration was positively correlated with the percentage of FoxP3 + Helios + double positive Treg at six months of post-recruitment period in the Tregs + RTX group ($r = 0.772$; $p = 0.013$) (Fig. 6C). The IL-1 receptor antagonist (IL-1Ra) was another anti-inflammatory cytokine upregulated in the sera of Tregs ($p < 0.001$) and Tregs + RTX ($p < 0.001$) patients, as compared to control ones ($p = 0.040$) throughout the follow-up (Fig. 6D). Notably, six months after recruitment, IL-1Ra serum concentration was fourteen-fold higher in Tregs patients and twelve-fold higher in Tregs + RTX patients than in the control group ($p < 0.001$). The phenomenon persisted until the end of the follow-up in Tregs + RTX patients, while it almost disappeared in the Tregs group at 24 months of the follow-up (Fig. 6D, black arrows). We then found a positive, weak correlation between the concentration of IL-1Ra and DDI/kg b.w. ($r = 0.671$; $p = 0.028$) at + 12 months and HbA1c ($r = 0.834$; $p = 0.009$) at + 24 months in the Tregs + RTX group (Figure S9).

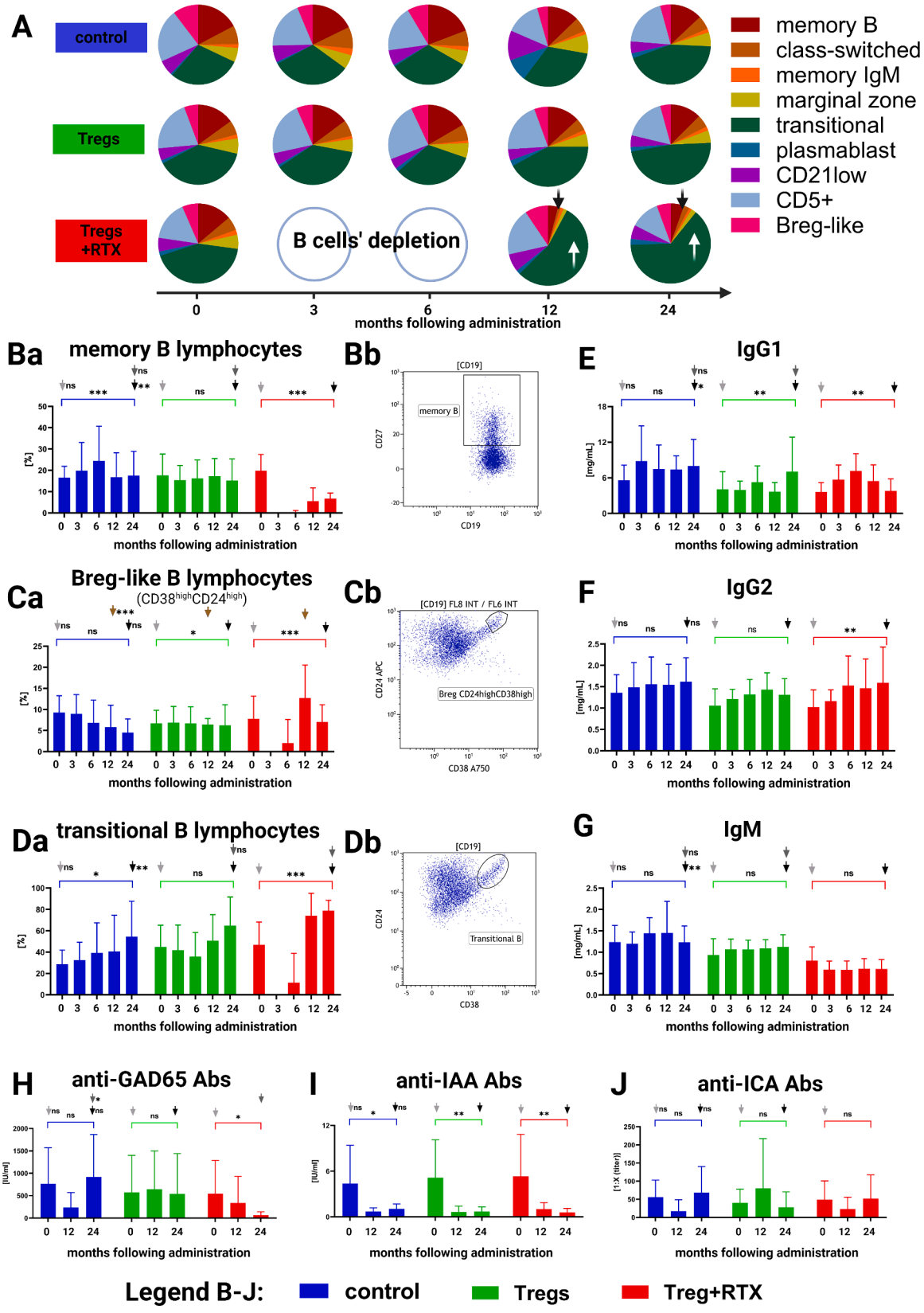

(caption on next page)

Fig. 4. Evolution of patients' humoral immune response up to two years post-therapy. Parts of whole diagrams for patients at administration, three, six, twelve, and twenty-four months after in a clinical trial **(A)** with colour-coded B cell phenotypes. In the Tregs + RTX group, the third and sixth month's observations are lacking due to the immunosuppressive rituximab effect. The percentages of CD27 antigen expression on B cells - memory B cells **(Ba)**; the percentages of $CD38^{high}/CD24^{high}$ antigen expression on B cells - Breg-like B cells **(Ca)**, and the percentages of CD38/CD24 antigen expression on B cells - transitional B cells **(Da)** are monitored throughout the clinical trial follow-up. A representative example of a cytogram with the gated population of interest is presented, memory B cells **(Bb),** Breg-like cells **(Cb),** and transitional B **(Db)**. The concentrations [mg/ml] of IgG1 **(E)**, IgG2 **(F)**, and IgM **(G)** are tracked throughout the clinical trial follow-up. The concentrations [IU/ml] of autoantibodies targeted against glutamic acid decarboxylase 65-kilodalton [GAD65] **(H)**, insulin [IAA] **(I)**, and titers for islet-cells [ICA] **(J)** are monitored throughout the clinical trial follow-up. In terms of statistical significance, Kruskal-Wallace for multiple comparisons and Mann-Whitney *U* test for comparison of two sets of data are used, and "NS" denotes non-significant, and significant p values are represented as follows: "***" (0.000–0.001), "**" (0.001–0.010), and "*" (0.010–0.050). The arrows denote the comparison between control, Tregs, and Tregs + RTX on administration (grey arrows), twenty-four months after (black arrows), for the highest numbers (brown arrows), or between 2 groups (dark grey arrows). The group numbers are 11/13/12 for control, Tregs, and Tregs + RTX in the clinical trial. For the Ba, Ca, Da, E, F, G, H, I, and J sub-panels charts, the bars represent means and line standard deviations.

In the case of proinflammatory cytokines, we have found a significant reduction in the concentrations of IL-17 throughout the study. While the levels of IL-17 were stable in the control samples throughout a 2-year-long follow-up ($p = 0.970$), they gradually decreased in the Tregs ($p = 0.003$) and the Tregs + RTX ($p = 0.006$) groups (Fig. 6E). In addition, there was a negative correlation between CD73 + CD4 + Teff and the concentration of IL-17 ($r = -0.694$, $p = 0.016$), noted at + 3 months in Tregs + RTX patients (Figure S10).

Another upregulated cytokine in the Tregs and the Tregs + RTX groups was the chemotactic factor IL-8/CXCL8. In control samples, IL-8/CXCL8 was comparable throughout a 2-year-long follow-up ($p = 0.590$), but in Tregs ($p = 0.040$) and Tregs + RTX ($p = 0.010$), an increased serum concentration was noted (Figure S11). A positive correlation between CD39 + FoxP3 + Treg and IL-8/CXCL8 serum concentration ($r = 0.615$, $p = 0.038$) occurred at + 6 months in the Tregs group (Figure S11).

The B cells class switching process was accompanied by the increased serum concentration of IL-4, IL-5 and soluble CD40 ligand (sCD40L) in the Tregs and the Tregs + RTX groups. The IL-4 was highly upregulated in the Tregs group from month + 3 to 2 years of the follow-up. In the case of IL-5, a peak in serum concentration occurred at + 6 months in Tregs + RTX patients ($p < 0.001$) (Figure S12). IL-4 positively correlated with serum IgG2 ($r = 0.767$, $p = 0.014$) in the Tregs + RTX group at + 12 months of the follow-up (Fig. 6F). Similarly, IL-5 was positively associated with serum IgG1 ($r = 0.753$, $p = 0.019$) in Tregs + RTX at + 12 post-recruitment months (Fig. 6G).

Unlike in the control or the Tregs groups, the serum concentration of sCD40L was upregulated in Tregs + RTX ($p = 0.040$), with the highest concentration at + 12 months (Figure S13). Moreover, sCD40L was positively correlated with DDI/kg b.w. ($r = 0.812$, $p = 0.021$) at the end of the trial (Figure S13).

4. Discussion

This study attempted to identify the most accurate immune biomarkers for the efficacy of therapy with Treg in DM1. In the TregVAC2.0 trial (clinical trial ISRCTN37116985), we followed immune parameters of cellular and humoral immunity and the cytokine network of newly diagnosed DM1 patients treated with combined therapy of autologous polyclonal Treg and anti-CD20 antibody. The data was compared to monotherapy with polyclonal Treg and control standard-of-care patients treated with insulin only. The study found that the increased percentage of PD-1 receptor (+) cells in CD4 + Treg, CD4 + Teff and CD8 + T cells from the peripheral blood was associated with favourable outcomes of therapy. In vitro, the higher percentage of PD-1 receptor (+) Treg correlated with better suppressive activity in functional suppression tests after stimulation for seven days. The effect disappeared on day 12, with a significantly reduced percentage of PD-1 receptor (+) CD4 + Treg in the culture. These correlations were not observed in the cultures of healthy controls. In addition, the B cell compartment was rebuilt toward a higher percentage of regulatory-like B cells at the expense of reduced memory B cells and the increased serum IgG2 at the cost of reduced serum concentration IgG1 in the group treated with combined therapy. These changes were accompanied by the reduced proinflammatory potential in the subjects receiving treatment compared to control patients, measured as increased concentrations of serum IL-10 and IL-1Ra and decreased concentrations of IL-17.

The most important observation of this study was that the administration of polyclonal Treg preserved the expression of the PD-1 receptor (+), and the combined therapy improved it even more, which may be a substantial therapeutic effect of this treatment. The percentages of PD-1 receptor (+) in T cells were higher in CD4 + Treg, CD4 + Teff and CD8 + T cells in DM1-treated patients compared to the DM1 control group at the end of the trial. Compared to the baseline, the expression of PD-1 receptor (+) was reduced in the DM1 control group, while remaining unaffected in the Tregs group and increased in the Tregs + RTX group. It was possible to calculate a PD-1 receptor (+) cut-off value for both regulatory and effector T cells to monitor therapy outcomes. The cut-off above 16 % for PD-1 receptor (+) Treg and > 8 % for PD-1 receptor (+) Teff pointed to the remission state in the Tregs + RTX group. Similarly, the cut-off above 7 % for CD73 + Tregs also was associated with better outcomes of the therapy. These calculations prove that Treg and Teff phenotypes can be applied for therapy response monitoring in particular individuals. We validated this observation in the in vitro model, comparing people with DM1 and healthy controls. This part of the study highlighted the highest importance of the expression of PD-1 receptor (+) on Treg in DM1. We found that the expression of this receptor on Treg and the percentage of PD-1 receptor (+) Treg increased significantly on day + 7, and the percentage dropped considerably on day + 12 in the cultures from DM1 patients. (Fig. 3D-G). Interestingly, in the cultures from DM1 patients, the suppressive potential of Treg in the suppression assay mainly correlated with the percentage of PD-1 receptor (+) Treg as it got boosted on day + 7 and significantly diminished on day + 12. No significant differences in the stimulated expression of PD-1 receptor (+) were found in the cultures of CD4 + Teff, and no associations were seen in the cultures of healthy controls. It may suggest that the expression of PD-1 receptor (+) on T cells wards off against autoimmunity in DM1. The disease is a stimulus which upregulates the expression of PD-1 receptor (+) similarly to the stimulation in vitro. Unfortunately, Treg from DM1 patients can upregulate PD-1 receptor (+) only transiently; therefore, the suppressive effect disappears quickly, and the disease may progress (Fig. 3H - I). It is an exciting observation in DM1 as the expression of PD-1 receptor (+) on activated T and B cells is known to control the function and proliferation of T cells [19,20]. Our study proves the link between this mechanism and protection from autoimmunity, such as DM1. There are reports that around one-third of cancer patients treated with PD-1/PD-L1 blocking antibodies developed immune-related adverse effects similar to autoimmune-like syndromes, for instance, autoimmune insulin-dependent diabetes [21,22]. Also, in nonobese diabetic mice, a model of DM1, the blockade of PD-1 receptor (+) pathway resulted in rapid diabetes progression [23]. Furthermore, it was shown that the PD-1/PD-L1 axis controls only the early phase of diabetogenic effector T cells in the pancreas, giving indirect proof that only early intervention could slow down disease progression [24]. A similar observation was made in systemic lupus erythematosus (SLE) patients treated with rituximab,

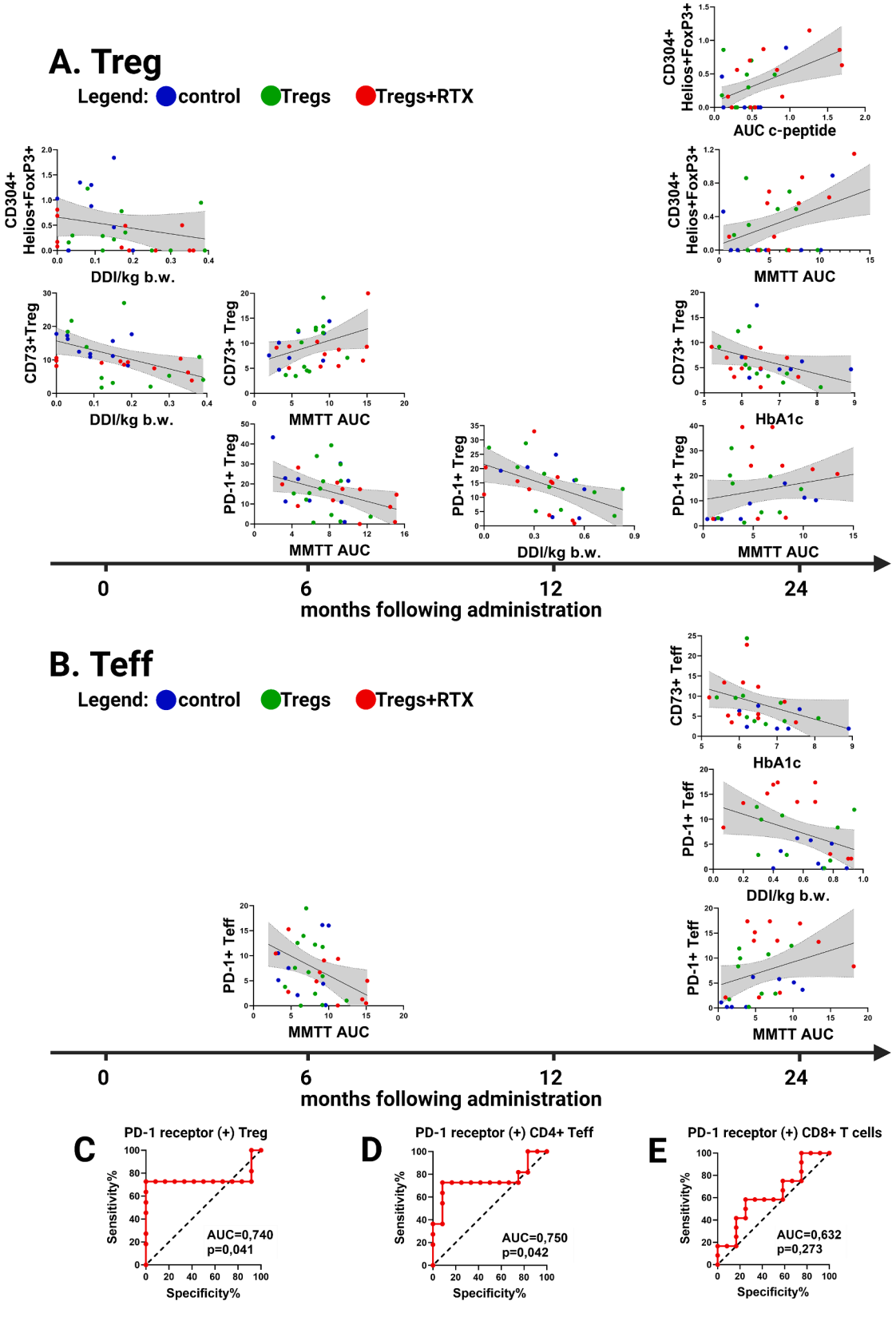

(caption on next page)

Fig. 5. Clinical correlates of regulatory T cells and effector T cells during patient follow-up. The correlation of PD-1 receptor (+), CD73, and CD304 markers expressed on Treg (A) and CD4 + effector T cells (Teff) (B) with clinical parameters, mixed-meal tolerance test (MMTT) assessed by area-under-curve of plasma C-peptide concentration (AUC), glycated haemoglobin (HbA1c), serum c-peptide, and daily dose insulin per kg of body weight (DDI/kg of b. w.). The statistical significance (p) and Spearman rank correlations (r) are presented in Table 2. Only statistically significant correlations are given, while others can be found in the supplementary data file (Figure S8). The green data dots represent the autologous Treg group (Tregs), red autologous Treg with rituximab group (Tregs + RTX), and blue standard therapy group (control). The group numbers are 11/13/12 for control, Tregs, and Tregs + RTX in the clinical trial. "Treg" stands for CD4 + regulatory T cells with FoxP3 intracellular expression, "Helios + FoxP3+" stands for CD4 + regulatory T cells with FoxP3 and Helios intracellular expression, and "CD4 + Teff" stands for CD4 effector T cells. The graphs visualise the percentages of antigens of interest on Treg cells or CD4 + Teff (y-axis) and the clinical feature (x-axis). Black lines indicate a correlation trend and dark-grey 95 % ellipse coefficient intervals. The values of antigen of interest are percentages (%), MMTT - stimulated C-peptide AUC240 (h*μg/L), fasting c-peptide (μg/L), HbA1c (%), DDI/kg b.w. In the C-E panels, AUC - area under the curve graphs with indicated AUC and p-values are presented for the sensitivity and specificity of PD-1 receptor (+) expression in FoxP3 + Treg (C), effector T cells (D), and CD8 + T cells (E).

Table 2
Statistically significant correlations of regulatory T cells' markers and CD4 + effector T cells with clinical parameters.

Time	Regulatory T cells		
	PD-1 receptor (+)	**CD73+**	**CD304+**
At administration		***vs. DDI/kg b. w.*** r=(−0.451) p = 0.007 (**)	***vs. DDI/kg b. w.*** r=(−0.349) p = 0.040 (*)
+6 months	***Vs. MMTT AUC*** r=(−0.345) p = 0.043 (*)	***Vs. MMTT AUC*** r = 0.346 p = 0.049 (*)	
+12 months	***vs. DDI/kg b. w.*** r=(−0.513) p = 0.004 (**)		
+24 months	***Vs. MMTT AUC*** r = 0.395 p = 0.038 (*)	***vs. HbA1c*** r=(−0.488) p = 0.006 (**)	***vs. c-peptide*** r = 0.394 p = 0.031 (*) ***vs. MMTT AUC*** r = 0.383 p = 0.037 (*)
Time	**Effector CD4 + T cells**		
	PD-1 receptor (+)	**CD73+**	
+ 6 months	***vs. MMTT AUC*** r=(−0.346) p = 0.049 (*)		
+24 months	***Vs. DDI/kg b.m.*** r=(−0.405) p = 0.033 (*) ***Vs. MMTT*** r = 0.444 p = 0.018 (*)	***vs. HbA1c*** r=(−0.488) p = 0.006 (**)	

The statistical significance (p) and Spearman rank correlations (r) values for correlation of PD-1 receptor (+), CD73, and CD304 markers expressed on Treg and CD4 effector T cells with clinical parameters, mixed-meal tolerance test (MMTT) assessed by area-under-curve of plasma C-peptide concentration (AUC), glycated haemoglobin (HbA1c), serum c-peptide, and daily dose insulin per kg of body weight (DDI/kg of b. w.). Only statistically significant correlations are provided, while others can be found in the supplementary data file (Figure S8). In terms of statistical significance, p values are represented as follows: "***" (0.000–0.001), "**" (0.001–0.010), and "*" (0.010–0.050).

where the percentage of CD4 + T cells with high PD-1 receptor (+) expression decreased in the follow-up, which was associated with disease progression [25]. Finally, the expression of PD-1 receptor (+) in our study was the most commonly correlated with the clinical markers of β-cell function, and we found several correlations for both treated and control patients. Moreover, the PD-1 receptor (+) associations were widespread for cell types (Treg, CD4 + Teff, and CD8 + T cells) and time points at follow-up (Fig. 5). The PD-1 receptor (+) upregulation was favourable for β-cell function, and as far as proved by the in-vitro model, its high expression correlated with the better suppressive function of Treg.

Another critical observation was that PD-1 receptor (+) expression was the highest in the Tregs + RTX group, which might be attributable to anti-CD20 treatment. In autoimmunity, like idiopathic thrombocytopenic purpura (ITP), rituximab was shown to increase the number of Treg and the expression of Fas ligand, mRNA levels of the proteins involved in apoptosis BAX and BCL2, restored Th1/Th2 ratio, and TCR Vβ clonality [26,27]. From the functional point of view, it was postulated that the depletion of CD20 + B cells changed T cells' activation in several pathways, among which decreased antigen presentation could be critical [28,29]. Similarly, in rheumatoid arthritis (RA) CD20 + B cell depletion reduced antigen-presenting cells (APC) pool and delayed autoimmunity, but only to a certain degree. Once B cells returned, antibody production and T cells' activation were restored, and the disease relapsed [30,31]. B cell depletion inhibited antigen-specific CD4 + T cell expansion in the mouse models of arthritis and autoimmune diabetes, giving another example that B cells were essential for T cell responses [32]. In the Tregs + RTX group B cell depletion resulted in an increased proportion of naïve, transitional, and regulatory-like B cells. Moreover, when the disease-specific autoantibodies were measured, the levels of anti-GAD65 persisted in the control and the Tregs groups but significantly reduced in the Tregs + RTX group (Fig. 4H). Furthermore, the Tregs + RTX group was characterised by increased levels of anti-inflammatory cytokines, especially IL-10 and IL-1Ra, and reduced serum concentration of IL-17. It was also true for the Tregs group, but only for continuing IL-17 reduction, while a time-dependent increase in IL-1Ra and IL-10 was not upheld (Fig. 6B - D). It is concordant with other reports in which rebuilding of B cell compartment with rituximab resulted in fewer autoreactive clones and more B cell subsets capable of IL-10 production, mainly transitional B cells [28].

In this light, our therapeutic strategy to combine rituximab with the administration of regulatory T cells is well-founded, as B cell depletion reduced antigen presentation, induced pro-tolerant B cell phenotype and anti-inflammatory cytokine milieu. At the same time, Treg reduced T cell proliferation and promoted anti-inflammatory response. The expression of PD-1 receptor (+) may thus be adopted as a biomarker of this immunomodulatory therapy as its upregulation predicts treatment effect (Fig. 3A, B).

A possible drawback of our study was the lack of a rituximab-treated-only DM1 group. It was widely due to the limited permission of the bioethical committee, which allowed us to carry out only combined treatment and make reference to the TN-05 trial by Pescovitz, who performed the study with rituximab earlier [33,34]. We had no real access to the samples from TN-05 trial patients, just to the results from a report which was published afterwards. Fortunately, there was plenty of evidence in the TN-05 trial on how B cell depletion shaped immunity in DM1. This trial showed that four doses of rituximab, a regimen similar to TregVAC2.0, preserved beta-cell function over one year, but when prolonged up to 30 months, no significant improvements could be found [33,34]. This finding was in opposition to our study, where rituximab was reinforced with the administration of polyclonal Treg, which resulted in the controlling of DM1 in terms of better results of MMTT and fasting C-peptide levels, DDI/kg b.w., HbA1c, remission and insulin independence at a two-year long follow up. The timing of B cell repopulation between six to twelve months after depletion (Figure S14) and persistently decreased serum IgM levels were similar between TN-05 and TregVAC2.0 (Fig. 4G). It should be noted that there is conflicting data in the literature on the effect of B cell depletion on the level of serum immunoglobulins. In the TN-05 trial, when compared to the control patients, DM1 patients treated with rituximab were characterised by comparable or increased serum total IgG concentration in the

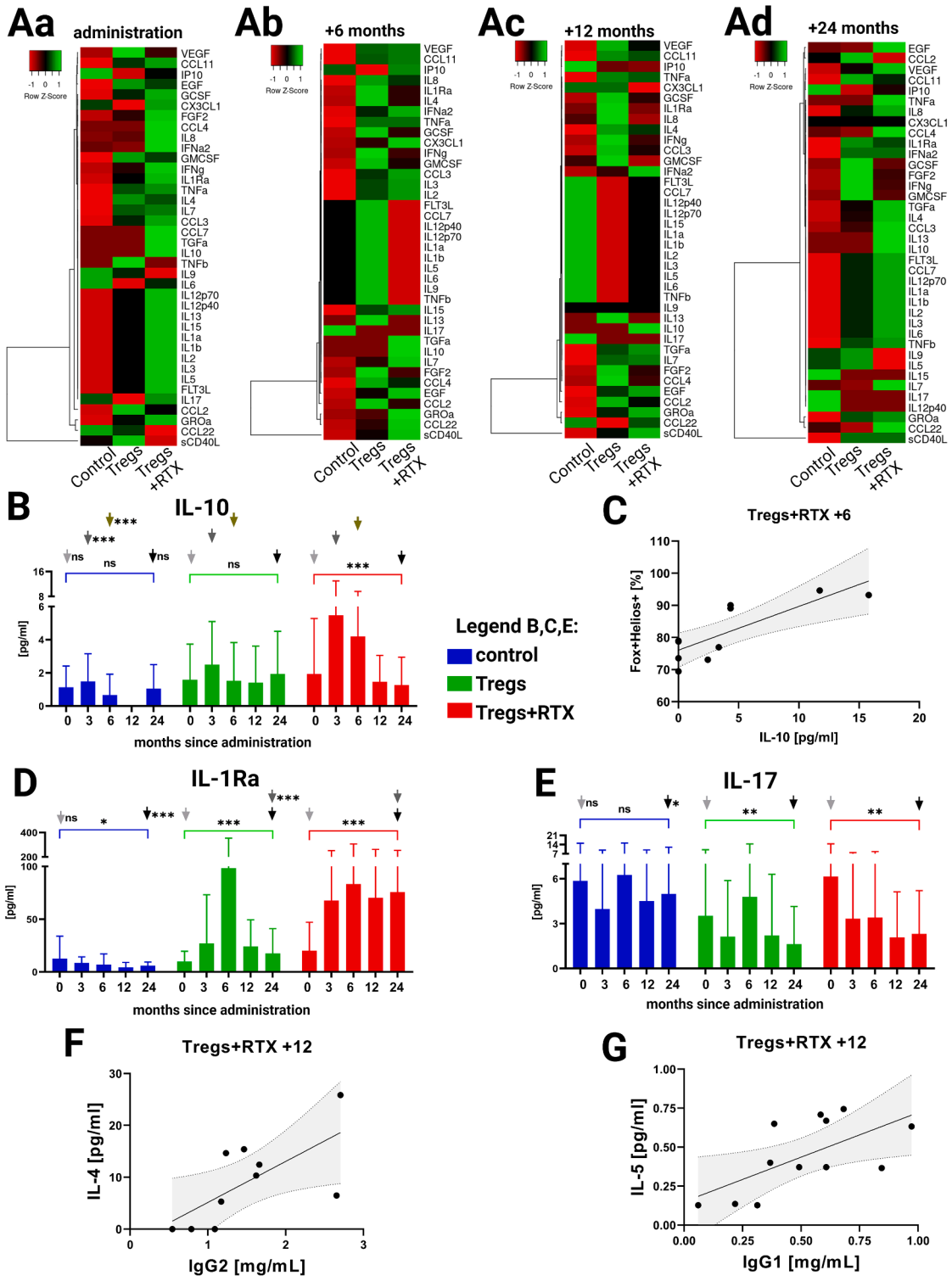

Fig. 6. Serum cytokines network during patient follow-up. The heatmap of cytokine serum concentration [pg/ml] is presented on administration **(Aa)**, six **(Ab)**, twelve **(Ac)**, and twenty-four **(Ad)** months after a clinical trial. The colour scale ranges from red indicating the lowest expression to green indicating the highest expression of antigens in the Treg population. The concentrations [pg/ml] of IL-10 **(B)**, IL-1Ra **(D)**, and IL-17 **(E)** are tracked throughout the clinical trial follow-up. Observations are made on Treg administration (light grey arrows), after three months (dark grey), after six months (brown arrows), and after twenty-four months (black arrows). In panel **(C)** the correlation of Helios + FoxP3 + [%] with IL-10 [pg/ml] is analysed six months following administration in Treg with rituximab patients. "Helios + FoxP3+" stands for CD4 + regulatory T cells with FoxP3 and Helios intracellular expression. In panels **(F)** and **(G)**, the correlation of IL-4 [pg/ml] with IgG2 [mg/ml] twelve months after administration and the correlation of IL-5 [pg/ml] with IgG1 [mg/ml] twelve months after administration in Treg with rituximab patients are presented. Black lines indicate a correlation trend and dark-grey 95 % ellipses coefficient intervals. In terms of statistical significance, the Kruskal-Wallace for multiple comparisons and the Mann-Whitney *U* test for comparison of two sets of data are used. Correlations are calculated with a simple linear regression model and non-parametric Spearman correlation. "NS" denotes non-significant, and significant p values are represented as follows: "***" (0.000–0.001), "**" (0.001–0.010), and "*" (0.010–0.050). In sub-panel charts, B, D, and E the group numbers are 11/13/12 for control, Tregs, and Tregs + RTX. The bars represent the mean values and line standard deviations.

longer follow-up [33,34]. Some reports showed unchanged post-rituximab serum IgG1, IgG2, IgG3, and IgG4 concentrations [35] or a selective decrease in serum IgG4 subclass only [36]. In our study, once B cells repopulated in Tregs + RTX patients, an increase in IgG2 at the expense of IgG1 occurred (Fig. 4E, F). It was concordant with the concentrations of the class-switching cytokines [37] as IgG1 serum concentration was positively correlated with peripheral IL-4 and IgG2 with IL-5 around 12 months post-rituximab (the time of B cell repopulation). The switch could directly affect IgG function as IgG1 binds complement and FcR receptors on monocytes and neutrophils more than IgG2 [38]. Hence, higher levels of IgG2 together with a higher percentage of regulatory-like B cells might contribute to better clinical outcomes in the Tregs + RTX group. Interestingly, it was reported in healthy individuals that serum IgG2 levels were negatively correlated with whole-body insulin sensitivity and muscle insulin sensitivity and associated with insulin-stimulated glucose disposal considering factors known to alter insulin sensitivity like age, gender, BMI, and others [39]. Obviously, changing levels of antibodies after B cell depletion with rituximab also affects immunity against infection. For example, after the flu vaccine in rituximab-treated rheumatoid arthritis patients, humoral response decreased in IgM, IgG1, and IgG3 levels. The phenomenon was time-dependent, observed only in the individuals depleted around one month before vaccination and abolished in individuals who were rituximab treated six to ten months earlier [40]. Although in our study, infections were observed in around 60 % of the Tregs + RTX group, it was comparable with the Tregs and the control groups [7].

To sum up, the efficacy of the combined therapy is attributable to several factors. In the study, it was mainly associated with an increasing percentage of PD-1 receptor (+) T cells (on Teff and CD8 + T cells in vivo and Treg in vivo and in vitro) and rebuilding of the B cell compartment towards tolerogenic phenotype. The expression of PD-1 receptors (+) on T cells may be a promising biomarker of the efficacy of this therapy. Our data gives a solid background for prospective immune monitoring in clinical trials and sheds light on the immunopathogenesis of DM1.

CRediT authorship contribution statement

Maciej Zieliński: Writing – review & editing, Writing – original draft, Visualization, Software, Methodology, Investigation, Formal analysis, Conceptualization. **Justyna Sakowska:** Writing – review & editing, Writing – original draft, Visualization, Software, Methodology, Investigation, Formal analysis, Conceptualization. **Dorota Iwaszkiewicz-Grześ:** Writing – review & editing, Methodology, Investigation. **Mateusz Gliwiński:** Writing – review & editing, Methodology, Investigation. **Matylda Hennig:** Writing – review & editing, Methodology, Investigation, Data curation. **Magdalena Żalińska:** Writing – review & editing, Methodology, Investigation, Data curation. **Anna Wołoszyn-Durkiewicz:** Writing – review & editing, Methodology, Investigation, Data curation. **Anna Jaźwińska-Curyłło:** Writing – review & editing, Methodology, Investigation, Data curation. **Halla Kamińska:** Writing – review & editing, Methodology, Investigation. **Radosław Owczuk:** Writing – review & editing, Methodology, Investigation. **Wojciech Młynarski:** Writing – review & editing, Methodology, Investigation, Conceptualization. **Przemysława Jarosz-Chobot:** Writing – review & editing, Methodology, Investigation, Conceptualization. **Artur Bossowski:** Writing – review & editing, Methodology, Investigation, Conceptualization. **Agnieszka Szadkowska:** Writing – review & editing, Methodology, Investigation, Conceptualization. **Wojciech Fendler:** Writing – review & editing, Methodology, Investigation, Conceptualization. **Iwona Beń-Skowronek:** Writing – review & editing, Methodology, Investigation, Conceptualization. **Agata Chobot:** Writing – review & editing, Methodology, Investigation, Conceptualization. **Małgorzata Myśliwiec:** Writing – review & editing, Methodology, Investigation, Conceptualization. **Janusz Siebert:** Writing – review & editing, Methodology, Investigation, Conceptualization. **Natalia Marek-Trzonkowska:** Writing – review & editing, Methodology, Investigation, Conceptualization. **Piotr Trzonkowski:** Writing – review & editing, Writing – original draft, Validation, Supervision, Resources, Project administration, Methodology, Investigation, Funding acquisition, Formal analysis, Data curation, Conceptualization.

Declaration of competing interest

The authors declare the following financial interests/personal relationships which may be considered as potential competing interests: NMT, MM and PT are co-inventors of patents related to the presented content and stakeholders of the POLTREG venture. The Medical University of Gdansk received payment for the license to the given content. The other authors declare that they have no competing interests.

Data availability

Data will be made available on request.

Acknowledgments

We would like to extend our gratitude to Mrs Anita Dobyszuk, Mrs Grażyna Gniłka, Mrs Lucyna Szumacher-Sharma and Mrs Justyna Drabik from the Medical University of Gdansk Medical Centre for their perfect assistance in laboratory and clinical procedures.

Funding

Medical Research Agency, Poland (grant no 2022/ABM/05/00001 - 00) and EU Horizon 2020 Framework Programme (grant no: 830559 TREG H2020-EIC-SMEInst2018-2020/H2020-SMEInst-2018-2020-2).

Appendix A. Supplementary data

Supplementary data to this article can be found online at https://doi.org/10.1016/j.intimp.2024.111919.

References

[1] M.A. Budd, M. Monajemi, S.J. Colpitts, S.Q. Crome, C.B. Verchere, M.K. Levings, Interactions between islets and regulatory immune cells in health and type 1 diabetes, Diabetologia. 64 (11) (2021) 2378–2388, https://doi.org/10.1007/S00125-021-05565-6.

[2] A. Raugh, D. Allard, M. Bettini, Nature vs. nurture: FOXP3, genetics, and tissue environment shape Treg function, Front. Immunol. 13 (2022) 4199, https://doi.org/10.3389/FIMMU.2022.911151/BIBTEX.

[3] B.O. Roep, The need and benefit of immune monitoring to define patient and disease heterogeneity, mechanisms of therapeutic action and efficacy of intervention therapy for precision medicine in type 1 diabetes, Front. Immunol. (2023) 14, https://doi.org/10.3389/FIMMU.2023.1112858.

[4] B.O. Roep, E. Montero, R. van Tienhoven, M.A. Atkinson, D.A. Schatz, C. Mathieu, Defining a cure for type 1 diabetes: a call to action, lancet. Diabetes. Endocrinol. 9 (9) (2021) 553–555, https://doi.org/10.1016/S2213-8587(21)00181-9.

[5] K.C. Herold, B.N. Bundy, S.A. Long, et al., An anti-CD3 antibody, teplizumab, in relatives at risk for type 1 diabetes, N. Engl. J. Med. 381 (7) (2019) 603–613, https://doi.org/10.1056/NEJMOA1902226.

[6] S. Dong, K.J. Hiam-Galvez, C.T. Mowery, et al., The effect of low-dose IL-2 and Treg adoptive cell therapy in patients with type 1 diabetes, JCI. insight. 6 (18) (2021), https://doi.org/10.1172/JCI.INSIGHT.147474.

[7] M. Zieliński, M. Żalińska, D. Iwaszkiewicz-Grześ, et al., Combined therapy with CD4+CD25highCD127− T regulatory cells and anti-CD20 antibody in recent-onset type 1 diabetes is superior to monotherapy: Randomized phase I/II trial, Diabetes, Obes. Metab. 24 (8) (2022) 1534–1543, https://doi.org/10.1111/DOM.14723.

[8] J.A. Bluestone, J.H. Buckner, M. Fitch, et al., Type 1 diabetes immunotherapy using polyclonal regulatory T cells, Sci. Transl. Med. 7 (315) (2015), https://doi.org/10.1126/scitranslmed.aad4134.

[9] N. Marek-Trzonkowska, M. Myśliwiec, A. Dobyszuk, et al., Therapy of type 1 diabetes with CD4(+)CD25(high)CD127-regulatory T cells prolongs survival of pancreatic islets - results of one -year-long follow-up, Clin. Immunol. 153 (1) (2014) 23–30, https://doi.org/10.1016/j.clim.2014.03.016.

[10] N. Marek-Trzonkowska, M.A. Wujtewicz, M. Myśliwiec, et al., Administration of CD4+CD25highCD127- regulatory T cells preserves β-cell function in type 1 diabetes in children, Diabetes. Care. 35 (9) (2012) 1817–1820, https://doi.org/10.2337/DC12-0038.

[11] P. Trzonkowski, R. Bacchetta, M. Battaglia, et al., Hurdles in therapy with regulatory T cells, Sci. Transl. Med. 7 (304) (2015), https://doi.org/10.1126/SCITRANSLMED.AAA7721.
[12] N. Marek, M. Bieniaszewska, A. Krzystyniak, et al., The time is crucial for ex vivo expansion of T regulatory cells for therapy, Cell. Transpl. 20 (11–12) (2011) 1747–1758, https://doi.org/10.3727/096368911X566217.
[13] N. Marek-Trzonkowska, K. Piekarska, N. Filipowicz, et al., Mild hypothermia provides Treg stability, Sci. Rep. 7 (1) (2017) 11915, https://doi.org/10.1038/s41598-017-10151-1.
[14] A.C. Belkina, C.O. Ciccolella, R. Anno, R. Halpert, J. Spidlen, J.E. Snyder-Cappione, Automated optimized parameters for T-distributed stochastic neighbor embedding improve visualization and analysis of large datasets, Nat. Commun. 10 (1) (2019), https://doi.org/10.1038/S41467-019-13055-Y.
[15] E. Amid, M.K. Warmuth, TriMap: Large-scale Dimensionality Reduction Using Triplets, December 2019.
[16] J.H. Levine, E.F. Simonds, S.C. Bendall, et al., Data-driven phenotypic dissection of AML reveals progenitor-like cells that correlate with prognosis, Cell. 162 (1) (2015) 184–197, https://doi.org/10.1016/j.cell.2015.05.047.
[17] S. Babicki, D. Arndt, A. Marcu, et al., Heatmapper: web-enabled heat mapping for all, Nucleic. Acids. Res. 44 (W1) (2016) W147–W153, https://doi.org/10.1093/nar/gkw419.
[18] Primary Immunodeficiency Diseases - Immunoglobulin Disorders | Choose the Right Test. https://arupconsult.com/content/immunoglobulin-disorders?_ga=2.163356788.958945285.1684150934-1231057015.1684150933&_gl=1*tlimzr*_ga*MTIzMTA1NzAxNS4xNjg0MTUwOTMz*_ga_Z8H49DQE4D*MTY4NDE1MDkzMy4xLjEuMTY4NDE1MTI0My4wLjAuMA.. Accessed May 15, 2023.
[19] A. Vecchione, R. Di Fonte, J. Gerosa, et al., Reduced PD-1 expression on circulating follicular and conventional FOXP3+ Treg cells in children with new onset type 1 diabetes and autoantibody-positive at-risk children, Clin. Immunol. (2020) 211, https://doi.org/10.1016/J.CLIM.2019.108319.
[20] C.G. Tucker, A.J. Dwyer, B.T. Fife, T. Martinov, The role of programmed death-1 in type 1 diabetes, Curr. Diab. Rep. 21 (6) (2021) 20, https://doi.org/10.1007/S11892-021-01384-6.
[21] J.A. Bluestone, M. Anderson, K.C. Herold, et al., Collateral damage: insulin-dependent diabetes induced with checkpoint inhibitors, Diabetes. 67 (8) (2018) 1471–1480, https://doi.org/10.2337/DBI18-0002.
[22] M.A. Postow, R. Sidlow, M.D. Hellmann, Immune-related adverse events associated with immune checkpoint blockade, N. Engl. J. Med. 378 (2) (2018) 158–168, https://doi.org/10.1056/NEJMRA1703481.
[23] M.E. Keir, S.C. Liang, I. Guleria, et al., Tissue expression of PD-L1 mediates peripheral T cell tolerance, J. Exp. Med. 203 (4) (2006) 883–895, https://doi.org/10.1084/JEM.20051776.
[24] I. Guleria, M. Gubbels Bupp, S. Dada, et al., Mechanisms of PDL1-mediated regulation of autoimmune diabetes, Clin. Immunol. 125 (1) (2007) 16–25, https://doi.org/10.1016/J.CLIM.2007.05.013.
[25] F. Faustini, N. Sippl, R. Stålesen, et al., Rituximab in systemic lupus erythematosus: transient effects on autoimmunity associated lymphocyte phenotypes and implications for immunogenicity, Front. Immunol. 13 (2022) 1494, https://doi.org/10.3389/FIMMU.2022.826152/BIBTEX.
[26] R. Stasi, G. Del Poeta, E. Stipa, et al., Response to B-cell–depleting therapy with rituximab reverts the abnormalities of T-cell subsets in patients with idiopathic thrombocytopenic purpura, Blood. 110 (8) (2007) 2924–2930, https://doi.org/10.1182/BLOOD-2007-02-068999.
[27] R. Stasi, N. Cooper, P.G. Del, et al., Analysis of regulatory T-cell changes in patients with idiopathic thrombocytopenic purpura receiving B cell–depleting therapy with rituximab, Blood. 112 (4) (2008) 1147–1150, https://doi.org/10.1182/BLOOD-2007-12-129262.
[28] N. Cooper, D.M. Arnold, The effect of rituximab on humoral and cell mediated immunity and infection in the treatment of autoimmune diseases, Br. J. Haematol. 149 (1) (2010) 3–13, https://doi.org/10.1111/J.1365-2141.2010.08076.X.
[29] N. Cooper, R. Stasi, S. Cunningham-Rundles, et al., The efficacy and safety of B-cell depletion with anti-CD20 monoclonal antibody in adults with chronic immune thrombocytopenic purpura, Br. J. Haematol. 125 (2) (2004) 232–239, https://doi.org/10.1111/J.1365-2141.2004.04889.X.
[30] J.C.W. Edwards, L. Szczepański, J. Szechiński, et al., Efficacy of B-cell-targeted therapy with rituximab in patients with rheumatoid arthritis, N. Engl. J. Med. 350 (25) (2004) 2572–2581, https://doi.org/10.1056/NEJMOA032534.
[31] P. Wehr, H. Purvis, S.C. Law, R. Thomas, Dendritic cells, T cells and their interaction in rheumatoid arthritis, Clin. Exp. Immunol. 196 (1) (2019) 12–27, https://doi.org/10.1111/CEI.13256.
[32] J.D. Bouaziz, K. Yanaba, G.M. Venturi, et al., Therapeutic B cell depletion impairs adaptive and autoreactive CD4+ T cell activation in mice, Proc. Natl. Acad. Sci. USA 104 (52) (2007) 20878–20883, https://doi.org/10.1073/PNAS.0709205105.
[33] M.D. Pescovitz, C.J. Greenbaum, H. Krause-Steinrauf, et al., Rituximab, B-lymphocyte depletion, and preservation of beta-cell function, N. Engl. J. Med. 361 (22) (2009) 2143–2152, https://doi.org/10.1056/NEJMOA0904452/SUPPL_FILE/NEJM_PESCOVITZ_2143SA1.PDF.
[34] M.D. Pescovitz, C.J. Greenbaum, B. Bundy, et al., B-Lymphocyte depletion with rituximab and β-cell function: two-year results, Diabetes. Care. 37 (2) (2014) 453–459, https://doi.org/10.2337/DC13-0626.
[35] M.S. Kavuru, A. Malur, I. Marshall, et al., An open-label trial of rituximab therapy in pulmonary alveolar proteinosis, Eur. Respir. J. 38 (6) (2011) 1361–1367, https://doi.org/10.1183/09031936.00197710.
[36] A. Khosroshahi, M.N. Carruthers, V. Deshpande, S. Unizony, D.B. Bloch, J.H. Stone, Rituximab for the treatment of IgG4-related disease: lessons from 10 consecutive patients, Medicine (Baltimore). 91 (1) (2012) 57–66, https://doi.org/10.1097/MD.0B013E3182431EF6.
[37] D.T. Avery, V.L. Bryant, C.S. Ma, M.R. de Waal, S.G. Tangye, IL-21-induced isotype switching to IgG and IgA by human naive B cells is differentially regulated by IL-4, Accessed November 15, 2018, J. Immunol. 181 (3) (2008) 1767–1779, http://www.ncbi.nlm.nih.gov/pubmed/18641314.
[38] R. Hamilton, D. Abmli, C. Mohan, The Human IgG Subclasses, Hum. IgG. Subclasses. (2001), https://doi.org/10.1016/C2009-0-00373-0.
[39] T.V. Fiorentino, E. Succurro, F. Arturi, et al., Serum IgG2 levels are specifically associated with whole-body insulin-mediated glucose disposal in non-diabetic offspring of type 2 diabetic individuals: a cross-sectional study, Sci. Rep. 8 (1) (2018), https://doi.org/10.1038/S41598-018-32108-8.
[40] J. Westra, S. Van Assen, K.R. Wilting, et al., Rituximab impairs immunoglobulin (Ig)M and IgG (subclass) responses after influenza vaccination in rheumatoid arthritis patients, Clin. Exp. Immunol. 178 (1) (2014) 40–47, https://doi.org/10.1111/CEI.12390.